ChemComm

Accepted Manuscript

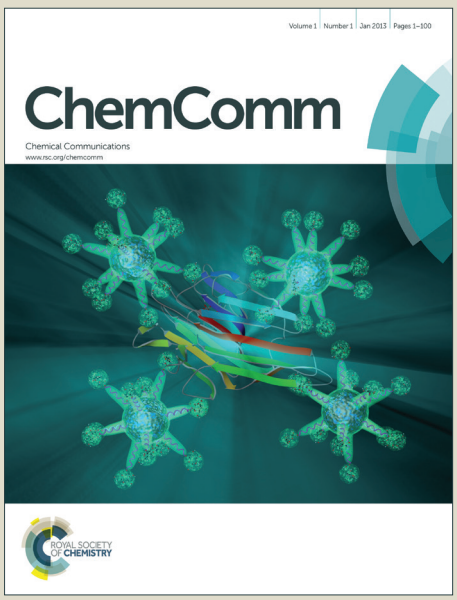

ROYAL SOCIETY OF CHEMISTRY

www.rsc.org/chemcomm

Journal Name

RSCPublishing

COMMUNICATION

A new type of carbon nitride-based polymer composite for enhanced photocatalytic hydrogen production

Cite this: DOI: 10.1039/x0xx00000x

Zheng Xing,[a] Zhigang Chen,[b] Xu Zong*[a] and Lianzhou Wang*[a]

Received 00th January 2014,
Accepted 00th January 2014

DOI: 10.1039/x0xx00000x

www.rsc.org/

A new type of graphitic C_3N_4–based composite photocatalysts were designed and prepared by co-loading PEDOT as hole transport pathway and Pt as electron trap on C_3N_4. The as-prepared C_3N_4-PEDOT-Pt composites showed drastically enhanced activity for visible light-driven photocatalytic H_2 production compared to those of C_3N_4-PEDOT and C_3N_4-Pt possibly due to the spatial separation of the reduction and oxidation reaction sites.

Photocatalytic hydrogen evolution using semiconductor materials provides a promising way to produce clean hydrogen fuel.[1] However, a significant factor limiting the overall photocatalytic efficiency is the rapid charge recombination after photo-excitation, which often happens during the diffusion of charges in the bulk as well as on the photocatalyst particle surface.[2, 3] In order to suppress the charge recombination, one effective solution is to design photocatalysts with spatially separated oxidative and reductive sites. For example, Kudo and co-workers prepared a NiO-loaded $NaTaO_3$ doped with lanthanum[4]. The Lanthanum doping induced the formation of nanostep structure on the surface of $NaTaO_3$ and H_2 evolution occurred on the NiO particles while O_2 evolution took place at the groove of the nanostep structure. Therefore, this type of catalysts exhibited high efficiency for overall water splitting into H_2 and O_2 under UV illumination due to the separation of the reduction and oxidation sites. Li et al. developed a dual cocatalyst system by loading Pt and PdS on CdS as the reduction and oxidation cocatalysts, respectively, and achieved impressively high quantum efficiency for hydrogen production.[5, 6] Recently, Li and co-workers found that the (010) and (110) facets of the $BiVO_4$ crystals are reductive and oxidative, respectively.[7, 8] Based on this finding, the selectively deposited reduction and oxidation catalysts on different facets led to much improved oxygen production upon visible light irradiation compared to $BiVO_4$ with randomly distributed cocatalyst. In this regard, the spatial separation of charge carriers in photocatalyst is significantly important for the photocatalytic efficiency.

Since the pioneer work on using graphitic carbon nitride (g-C_3N_4) for photocatalytic water splitting reported by Wang et al.[9], g-C_3N_4, a polymer semiconductor has drawn great attention as a promising photocatalyst due to its visible light absorption, suitable band position for both H_2 and O_2 production, and relatively good thermal and chemical stability.[10] However, the photocatalytic activities of pure g-C_3N_4 are still limited due to the serious charge recombination, and much effort has been devoted to addressing this issue.[11-16]

Poly (3, 4-ethylenedioxythiophene) (PEDOT) has been recognised to be an excellent conducting polymer in optoelectronic devices because PEDOT possesses excellent conductivities, thermal stability, transparency in the visible range and the ability to be processed in aqueous solution.[17, 18] For instance, as a result of its high hole mobility, PEDOT is often exploited as hole conductor in Dye Sensitized Solar Cells (DSSCs).[18, 19] Moreover, PEDOT has been used to not only conduct holes but also catalyse water oxidation reaction in the configuration of photoelectrochemical cells.[20] Considering the aforementioned outstanding electrical, chemical, catalytic and optical properties of PEDOT, we wonder whether it is possible to construct a C_3N_4-PEDOT composite and use PEDOT as a hole transport pathway. Furthermore, as Pt particles are often deposited onto g-C_3N_4 as proton reduction sites, we may create a C_3N_4-PEDOT-Pt system, in which PEDOT and Pt act as oxidation and reduction reaction sites, respectively. Herein, we report a new type of C_3N_4 composite photocatalyst by co-loading PEDOT and Pt cocatalysts on C_3N_4. The as-prepared C_3N_4-PEDOT-Pt photocatalyst produced 4 times more hydrogen than conventional C_3N_4-Pt photocatalyst under optimized conditions. The speculated spatial separation of the reductive and oxidative reaction sites on C_3N_4 can efficiently suppress the recombination of photogenerated electrons and holes and was considered to be the main reason for the drastically enhanced photocatalytic performance.

The C_3N_4-PEDOT-Pt composites were prepared by co-loading PEDOT and Pt particles on g-C_3N_4 using a two-step method (Scheme 1, see ESI† for experimental details). Commercially available poly(3,4-ethylenedioxythiophene):poly(styrenesulfonate) (PEDOT-PSS) complex was used, in which the PSS has dual functions of acting as the counterion of the positively charged PEDOT and rendering the dispersibility in aqueous medium.[21] In the first step, different amounts of PEDOT-PSS were loaded on g-C_3N_4 by impregnating g-C_3N_4 in commercial PEDOT-PSS solution. As PEDOT-PSS is soluble in water, the resulting C_3N_4-PEDOT composite was post-treated with ethylene glycol (EG) to avoid the detachment of the PEDOT in aqueous solution.[22] Moreover, treatment with EG can improve the conductivity and stability of

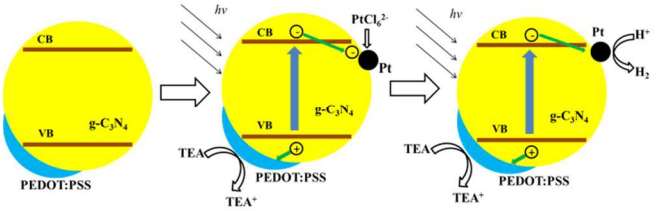

Scheme 1 Schematic of the preparation process of the C_3N_4-PEDOT-Pt composite and the proposed mechanism of the photocatalytic reaction.

PEDOT.[17, 22] In the second step, Pt nanoparticles were loaded on the C_3N_4-PEDOT composite powder via an in-situ photoreduction method in the presence of a hole scavenger.

The X-ray diffraction (XRD) pattern of as-prepared g-C_3N_4 (Fig. S1a, ESI†) shows two peaks: a low-angle (100) peak at around 15.3° corresponding to the tri-s-triazine units packing in the lattice planes parallel to the c-axis, and a (002) peak at around 32.1° stemmed from the periodic stacking of individual layers.[11, 16] XRD patterns of C_3N_4-PEDOT composites with different ratios of PEDOT are very similar to that of g-C_3N_4, indicating that the addition of PEDOT made insignificant change to the crystal structure of g-C_3N_4 (Fig. S1b-e, ESI†). The optical absorption properties of all samples were then examined by UV-visible spectroscopy. The g-C_3N_4 has an absorption edge at 466 nm, corresponding to a band gap of 2.66 eV (Fig. S2a, ESI†). After the impregnation of PEDOT, the absorption edge of g-C_3N_4 remained nearly unchanged while the baseline was elevated (Fig. S2b-e, ESI†). This phenomenon reveals that PEDOT did not change the electronic structure of g-C_3N_4. The rise of absorption baseline by PEDOT is reflected by the gradual colour change of C_3N_4-PEDOT from yellow (pure g-C_3N_4) to dark green (C_3N_4-5 wt% PEDOT) with the increase of the ratios of PEDOT.

The morphology of C_3N_4-PEDOT composite was investigated with transmission electron microscopy (TEM). The g-C_3N_4 possessed a layered structure (Fig. 1a and Fig. S3). To confirm the presence of PEDOT in the polymer composite and determine the distribution of PEDOT, element mapping analysis was conducted. As shown in Fig.1 b-e, all C, N, O and S elements are evenly distributed at the surface of C_3N_4-5 wt% PEDOT. S elements only come from the C-S-C in the PEDOT and sulfonic acid or sulfonate functional groups in the PSS, while O elements only come from sulfonic acid or sulfonate functional groups in the PSS. The distribution of S and O elements indicates that the surface of g-C_3N_4 was relatively uniformly covered by the PEDOT-PSS polymer.

To further confirm the existence of PEDOT on C_3N_4, X-ray photoelectron spectroscopy (XPS) analysis was performed. Similar results in the XPS spectra of S 2p of all C_3N_4-PEDOT samples were observed (Fig. S4, ESI†). The lower binding energy peaks at 163.5 eV and 164.7 eV can be assigned to sulphur atoms in PEDOT while the higher binding energy peak at 168.8 eV corresponds to S atoms in PSS.[23] Moreover, the ratio of PEDOT to PSS is estimated to be around 1:3 based on the measured area ratio of PEDOT to PSS in the S 2p spectra, which is in good agreement with previous reports .[23, 24]

We then investigated the photocatalytic H_2 evolution performance of the composites. Fig. 2A shows the H_2 evolution rates of all samples under visible light illumination. When loaded with Pt, pure g-C_3N_4 (Fig. 2A-a) can only produce H_2 at a rate of 6.4 μmol h^{-1} in the first 4 h. With the increase of the amount of PEDOT, the hydrogen production rate steadily rose, reaching a maximum at 2 wt% loading. C_3N_4-2 wt% PEDOT (Fig. 2A-d) showed a hydrogen evolution rate of 32.7 μmol h^{-1}, which was over 4 times higher than that of g-C_3N_4. However, when the loading was increased to to 5 wt%, the activity decreased (Fig. 2A-e). All the C_3N_4-PEDOT-Pt composites exhibited much improved H_2 evolution compared to g-C_3N_4-Pt in aqueous triethanolamine (TEA) solution. In a control

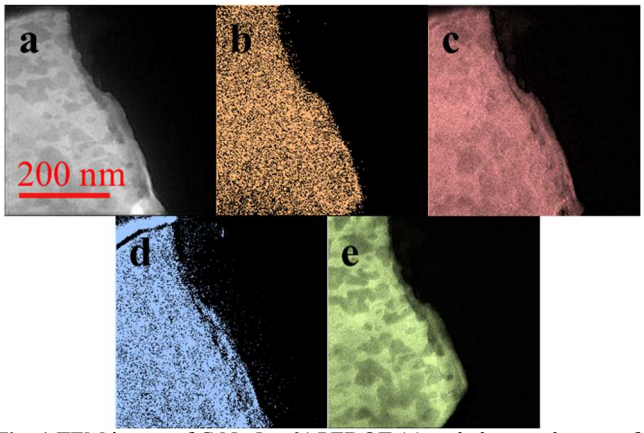

Fig. 1 TEM image of C_3N_4-5 wt% PEDOT (a) and elemental maps of C (b), N (c), O (d) and S (e).

experiment, we also tested the H_2 evolution on C_3N_4 without Pt, and only negligible amount of H_2 was detected when using C_3N_4-2 wt% PEDOT (Fig. 2A-f). The results indicate that PEDOT cannot work as the reduction reaction site like Pt. Moreover, PEDOT by itself was not able to produce any H_2 in TEA solution regardless of the presence of Pt (not shown in the Fig. 2). This indicates that PEDOT cannot act as the light absorber to induce photocatalytic H_2 production.

In order to investigate the origin of the difference of the photocatalytic performance and the role of PEDOT, photoluminescence (PL) analysis was performed. Fig. 3 shows the PL spectra of g-C_3N_4 and PEDOT-C_3N_4 composites. The broad peaks at around 460 nm are related to the electron-hole recombination in g-C_3N_4,[13, 16] and the peak position agrees well with the band gap (2.66 eV) of g-C_3N_4. When the PEDOT loading was increased, the PL peak became gradually quenched. The weakened PL signals with the increased PEDOT loading implied the decreased electron-hole recombination, which led to the improved H_2 evolution. Theoretically, as PEDOT is a hole conductor, photogenerated electrons will not transfer from g-C_3N_4 to PEDOT and therefore Pt cannot form on the PEDOT surface. Instead, $PtCl_6^{2-}$ ions can only be reduced to Pt on the bare surface of g-C_3N_4 where PEDOT is not present (Scheme 1). Therefore, reduction (Pt) and oxidation (PEDOT) reaction sites should be spatially separated on the surface of g-C_3N_4 through the present two-step method. Such a structure will facilitate charge separation and is supposed to lead to enhanced photocatalytic performance. This speculation is further confirmed by the quenching of PL signal upon photodeposion of Pt on C_3N_4-PEDOT (Fig. 3B). It is worth noting that even though C_3N_4-5 wt% PEDOT has the weakest PL peak, when loaded with Pt it produced less H_2 than C_3N_4-2 wt% PEDOT- 1 wt% Pt and C_3N_4-1 wt% PEDOT- 1 wt% Pt. We believe that when the PEDOT loading was too high, the available surface sites for $PtCl_6^{2-}$ reduction were limited, and so the lessened Pt sites led to drop in hydrogen production. We attempted to use TEM to acquire the direct evidence on the spatial separation of the reduction (Pt) and oxidation (PEDOT) reaction sites on C_3N_4, unfortunately no desirable results were obtained due to the low contrast between PEDOT and C_3N_4. However, from the synthesis process illustrated in Scheme 1 and our discussion above, we tend to consider that spatial separation of Pt and PEDOT should be the main reason for the high photocatalytic activity of the composite, while detailed mechanism study still needs further investigations.

To test the stability of C_3N_4-PEDOT in the aqueous reaction environment, a 12-hour cycle experiment was carried out with C_3N_4-2 wt% PEDOT. During the reaction, the reaction system was re-

evacuated every 4 hours and illumination was resumed after re-evacuation. As shown in Fig. 2B, the activity was well maintained after 12 hours and the catalyst can produce a total amount of 452.77 μmol of H_2. Moreover, it is noticed that the second and third cycles witnessed slightly increased H_2 evolution than the first cycle, possibly due to the photodeposition of Pt particles in the beginning of photocatalytic reaction. In previous reports about C_3N_4-polymer composites, H_2 evolution always suffered decay after prolonged reaction time possibly due to photocorrosion.[11, 12] The remarkably improved stability of our C_3N_4-PEDOT composites can be attributed to the stability of PEDOT and the intimate contact between PEDOT and g- C_3N_4.

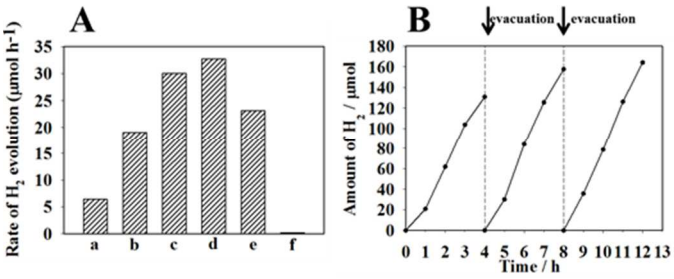

Fig. 2 H_2 evolution performance on different samples. A: rates of photocatalytic H_2 evolution in the first 4 hours on (a) pure g-C_3N_4, C_3N_4-PEDOT with PEDOT loading of (b) 0.5 wt%, (c) 1 wt%, (d) 2 wt%, and (e) 5 wt% and (f) C_3N_4-2 wt% PEDOT without Pt. B: the time course of H_2 evolution in a 12-hour cycle experiment on C_3N_4-2 wt% PEDOT. In all experiments, 0.1g of catalyst was loaded with 1 wt% Pt as the cocatalyst except (f) in A. 300 mL of triethanolamine (TEA) aqueous solution (10 vol%) was used as the reaction solution. High energy Xenon lamp equipped with 400 nm cut-off filter was used as the light source.

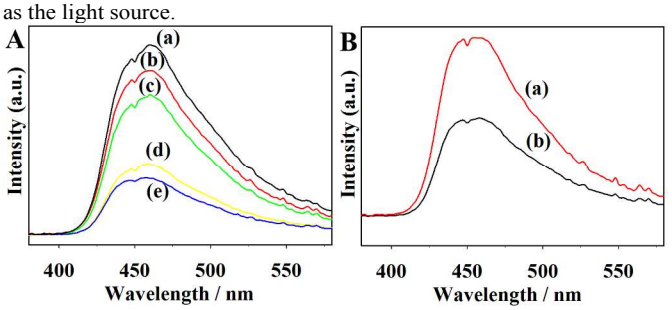

Fig. 3 The PL spectra of pure g-C_3N_4 and C_3N_4-PEDOT composites. A: PL spectra of all samples before photocatalytic reaction: (a) pure g-C_3N_4, C_3N_4-PEDOT with PEDOT loading of (b) 0.5 wt%, (c) 1 wt%, (d) 2 wt% and (e) 5 wt%. B: PL spectra of C_3N_4-2 wt% PEDOT (a) before and (b) after photocatalysis reaction with photodeposited Pt particles.

Conclusions

In summary, a new type of C_3N_4-based composite photocatalysts loaded with dual cocatalysts Pt and PEDOT have been developed. The as-prepared composites exhibited very stable and drastically enhanced photocatalytic hydrogen production compared to pure g-C_3N_4 under visible light illumination. The excellent performance of the composites can be attributed to the spatial separation of the reduction and oxidation reaction sites on C_3N_4. This finding demonstrates the important role of hole-conducting polymer for the generation of specially separated reductive and oxidative sites toward more efficient photocatalysis, and this concept could also be applied to other semiconductor-based photocatalyst systems.

This project was supported by Australian Research Council (through its DP and Future Fellowship programs).

Notes and references

[a] Nanomaterials Centre, School of Chemical Engineering and AIBN, The University of Queensland, Qld 4072, Australia. Fax: +61 7 33654199; Tel: +61 7 3365218; E-mail: l.wang@uq.edu.au; x.zong@uq.edu.au
[b] Materials Engineering, The University of Queensland, QLD 4072, Australia.

Electronic Supplementary Information (ESI) available: details of experimental procedures and characterizations (XRD, UV-Vis, XPS, etc.). See DOI: 10.1039/c000000x/

1. A. Kudo and Y. Miseki, *Chem. Soc. Rev.*, 2008, **38**, 253-278.
2. G. Liu, L. Wang, H. G. Yang, H. M. Cheng and G. Q. M. Lu, *J. Mater. Chem.*, 2009, **20**, 831-843.
3. F. E. Osterloh, *Chem. Mat.*, 2007, **20**, 35-54.
4. H. Kato, K. Asakura and A. Kudo, *J. Am. Chem. Soc.*, 2003, **125**, 3082-3089.
5. J. Yang, H. Yan, X. Wang, F. Wen, Z. Wang, D. Fan, J. Shi and C. Li, *J. Catal.*, 2012, **290**, 151-157.
6. J. Yang, D. Wang, H. Han and C. Li, *Acc. Chem. Res.*, 2013, **46**, 1900-1909.
7. R. Li, F. Zhang, D. Wang, J. Yang, M. Li, J. Zhu, X. Zhou, H. Han and C. Li, *Nat. Commun.*, 2013, **4**, 1432.
8. R. Li, H. Han, F. Zhang, D. Wang and C. Li, *Energy Environ. Sci.*, 2014.
9. X. Wang, K. Maeda, A. Thomas, K. Takanabe, G. Xin, J. M. Carlsson, K. Domen and M. Antonietti, *Nat. Mater.*, 2009, **8**, 76-80.
10. Y. Wang, X. Wang and M. Antonietti, *Angew. Chem., Int. Ed.*, 2012, **51**, 68-89.
11. Y. Sui, J. Liu, Y. Zhang, X. Tian and W. Chen, *Nanoscale*, 2013, **5**, 9150-9155.
12. H. Yan and Y. Huang, *Chem. Commun.*, 2011, **47**, 4168-4170.
13. Y. Hou, Z. H. Wen, S. M. Cui, X. R. Guo and J. H. Chen, *Adv. Mater.*, 2013, **25**, 6291-6297.
14. D. H. Wang, Y. W. Zhang and W. Chen, *Chem. Commun.*, 2014, **50**, 1754-1756.
15. Y. B. Li, H. M. Zhang, P. R. Liu, D. Wang, Y. Li and H. J. Zhao, *Small*, 2013, **9**, 3336-3344.
16. P. Niu, L. L. Zhang, G. Liu and H. M. Cheng, *Adv. Funct. Mater.*, 2012, **22**, 4763-4770.
17. J. Ouyang, C. W. Chu, F. C. Chen, Q. Xu and Y. Yang, *Adv. Funct. Mater.*, 2005, **15**, 203-208.
18. A. J. Mozer, D. K. Panda, S. Gambhir, B. Winther-Jensen and G. G. Wallace, *J. Am. Chem. Soc.*, 2010, **132**, 9543-9545.
19. X. Liu, Y. Cheng, L. Wang, L. Cai and B. Liu, *Phys. Chem. Chem. Phys.*, 2012, **14**, 7098-7103.
20. X. Li, W. Lu, W. Dong, Q. Chen, D. Wu, W. Zhou and L. Chen, *Nanoscale*, 2013, **5**, 5257-5261.
21. S. Kirchmeyer and K. Reuter, *J. Mater. Chem.*, 2005, **15**, 2077-2088.
22. J. K. Lee, J. M. Cho, W. S. Shin, S. J. Moon, N. T. Kemp, H. Zhang and R. Lamb, *J. Korean Phys. Soc.*, 2008, **52**, 621-626.
23. J. Kim, J. Jung, D. Lee and J. Joo, *Synth. Met.*, 2002, **126**, 311-316.
24. G. Greczynski, T. Kugler and W. R. Salaneck, *Thin Solid Films*, 1999, **354**, 129-135.